Inhibition of Chymotrypsin by Peptidyl Trifluoromethyl Ketones: Determinants of Slow-Binding Kinetics†

Kenneth Brady‡ and Robert H. Abeles*,§

Department of Toxicology, Harvard School of Public Health, 665 Huntington Avenue, Boston, Massachusetts 02115, and Graduate Department of Biochemistry, Brandeis University, 415 South Street, Waltham, Massachusetts 02254

Received December 27, 1989; Revised Manuscript Received May 2, 1990

ABSTRACT: A series of seven peptidyl trifluoromethyl ketone (TFK) inhibitors of chymotrypsin have been prepared which differ at the P_1 and P_2 subsites. Inhibition equilibria and kinetics of association and dissociation with chymotrypsin have been measured. The association rate of Ac-Phe-CF_3 was measured at enzyme concentrations between 8 nM and 117 μM in order to examine the relation between the ketone/hydrate equilibrium of trifluoromethyl ketones and the "slow binding" by these inhibitors. The association rate decreases at high enzyme concentrations, indicating that TFK ketone is the reactive species and that conversion of TFK hydrate to ketone becomes rate limiting under these conditions. Inhibitors with hydrophobic side chains at P_2 bind more tightly but more slowly to chymotrypsin, indicating that formation of van der Waals contacts between the P_2 side chain and the His 57 and Ile 99 side chains of chymotrypsin is a relatively slow process. Inhibitor properties were compared to the Michaelis–Menten kinetic constants of a homologous series of peptide methyl ester and peptide amide substrates. Plots of log K_i vs log (k_{cat}/K_m) are linear with slopes of 0.65 ± 0.2, indicating that these inhibitors are able to utilize 65% of the total binding energy between chymotrypsin and its hydrolytic transition state.

Peptidyl aldehydes (Stein & Strimpler, 1987), boronic acids (Kettner & Shenvi, 1984), and trifluoromethyl ketones (Imperiali & Abeles, 1986) are being studied as potent inhibitors of serine proteases. Each class of inhibitor is described as a "transition-state analogue" on the basis of the similarities of the enzyme–inhibitor complexes to the covalent, tetrahedral, zwitterionic adduct which is believed to be a high-energy transient species occurring during the enzyme-catalyzed hydrolysis of substrates (Fersht & Requena, 1971a). The study of these inhibitors is of interest both for the possible development of therapeutic agents and for the enhancement of our understanding of the basic mechanisms by which enzymes effect catalysis. Work in this laboratory has focused on the study of peptidyl trifluoromethyl ketones by use of NMR (Liang & Abeles, 1987), crystallographic (Brady et al., 1990), and kinetic (Brady et al., 1989) methods.

The dipeptidyl trifluoromethyl ketone Ac-Leu-Phe-CF_3[1] reacts with chymotrypsin slowly, with a second-order association rate constant of 800 M^{-1} s^{-1} at pH 7.0, while the monopeptidyl trifluoromethyl ketone Ac-Phe-CF_3 reacts with chymotrypsin at a rate too fast to be measured by steady-state kinetic methods (Imperiali & Abeles, 1986). Crystallographic studies of the chymotrypsin–Ac-Leu-Phe-CF_3 and chymotrypsin–Ac-Phe-CF_3 complexes (Brady et al., 1990) reveal no differences in enzyme conformation between these complexes which would correlate with the different kinetic behaviors. The crystallographic structure of the chymotrypsin–Ac-Leu-Phe-CF_3 complex identifies a close van der Waals contact between the P_2[2] leucine side chain of Ac-Leu-Phe-CF_3 and the His 57 imidazole of chymotrypsin. This interaction between a catalytically active residue and a portion of inhibitor remote from the hydrolytic center may be important in determining association kinetics.

The systematic variation of the P_2 subsite of substrates and peptidyl TFK inhibitors therefore seemed a promising means of examining the source of the "slow-binding" kinetics observed with Ac-Leu-Phe-CF_3 and of characterizing a strong, catalytically relevant van der Waals interaction between enzyme and substrate/inhibitor. Studies of the interaction at P_2 may also help to define the transition-state character of the enzyme–TFK complexes. Kinetic characterization of a series of mono- and dipeptide methyl esters, amides, and trifluoromethyl ketones are presented with these goals.

Materials and Methods

Materials

Chymotrypsin (3× recrystallized), *N*-benzoyl-L-tyrosine ethyl ester (BTEE), succinyl-L-alanyl-L-alanyl-L-prolyl-L-phenylalanyl *p*-nitroanilide (SAAPFpNA), isobutyl chloroformate, and *N*-methylmorpholine (NMM) were obtained from Sigma Chemical Co. Amino acids and amino acid amides and esters were purchased from either Sigma or Chemical Dynamics. Raney nickel, Dess Martin reagent, triphenylphosphine, 2-(2-hydroxyethyl)naphthalene, (2-bromoethyl)-benzene, *N*-bromosuccinimide, and dimethyl sulfoxide were purchased from Aldrich. Trifluoroacetaldehyde ethyl hemiacetal was purchased from Fairfield Chemical. Anhydrous potassium carbonate, sodium nitrite, sodium thiosulfate, and

† Publication No. 1712 of the Graduate Department of Biochemistry, Brandeis University. This research is supported by NIH Grant GM 12633-27 to R.H.A.

* Address correspondence to this author.
‡ Harvard School of Public Health.
§ Brandeis University.

[1] Phe-CF_3 denotes the trifluoromethyl ketone analogue of L-phenylalanine. Np-CF_3 denotes 1,1,1-trifluoro-3-amino-4-(2-naphthyl)-2-butanone. Other abbreviations: TFK, trifluoromethyl ketone; BTEE, *N*-benzoyl-L-tyrosine ethyl ester; SAAPFpNA, succinylalanylalanylprolylphenylalanine *p*-nitroanilide.

[2] The nomenclature of Schechter and Berger (1967) is used to specify interactions between the protease and bound peptides. Amino acid residues of substrates are numbered P_1, P_2, etc. toward the N-terminal direction and P_1', P_2', etc. toward the C-terminal direction from the scissile bond.

0006-2960/90/0429-7608$02.50/0

ACS-grade solvents (acetonitrile, ethyl acetate, methanol, diethyl ether, tetrahydrofuran, and methylene chloride) were obtained from Fisher Scientific.

Buffers used were 100 mM potassium phosphate, pH 7.0 (buffer A), and 0.1 mM potassium phosphate plus 100 mM potassium sulfate, pH 7.0 (buffer B for pH-state assays). All buffer salts were purchased from Fisher Scientific.

Synthesis of Substrates

Procedures used for the acetylation of amino acids, preparation of methyl esters, and couplings via the mixed-anhydride method are described in detail in the supplementary material (see paragraph at end of paper regarding supplementary material). The identity and purity of all mono- and dipeptide substrates were ascertained by ^1H and ^{13}C NMR and by TLC in at least two solvent systems. Details of purification procedures and NMR spectra are available in the supplementary material.

N-Acetyl-L-valyl-L-phenylalaninamide is an intractable solid of limited solubility in any common solvent. The purified product was pure to the limit of detection by ^1H and ^{13}C NMR but retained a ninhydrin-positive polar impurity detectable by TLC. It has been assumed that this substance is entrained *N*-methylmorpholinium chloride or residual valinamide, which would not significantly interfere with the amide hydrolysis assay.

All methyl ester substrates and most amide substrates were freely soluble in acetonitrile. UV absorbance spectra between 300 and 235 nm indicated characteristic bands resulting from the phenyl ring of phenylalanine or the indole ring of tryptophan. The concentrations of phenylalanine-based substrate solutions were evaluated from the absorbance maximum at 257 nm with an absorption coefficient of 177 M^{-1}. The concentration of tryptophan-based substrate solutions was evaluated from the absorbance maximum at 279 nm with an absorption coefficient of 5248 M^{-1}.

Synthesis of Inhibitors

Two trifluoromethyl amino alcohols, 1,1,1-trifluoro-3-amino-4-phenyl-2-butanol and 1,1,1-trifluoro-3-amino-4-(2-naphthyl)-2-butanol, were prepared as precursors to peptidyl trifluoromethyl ketones. Synthesis of the former compound was by the method of Imperiali and Abeles (1986). The latter compound was synthesized by analogous methods. These procedures, as well as further couplings, oxidations, and purifications, are described in the supplementary material.

Enzyme Assays

Spectrophotometric BTEE Assay. Assays were conducted in 1.0 mL of buffer A containing 500 μM *N*-benzoyl-L-tyrosine ethyl ester (BTEE) and 2.5% (v/v) acetonitrile. Hydrolysis of BTEE was initiated by addition of enzyme in a 5–25-μL aliquot, giving final concentrations in the range of 1–50 nM chymotrypsin. The absorbance of the assay solution was monitored at 256 nm, and the rate of BTEE hydrolysis was calculated from the increase in the molar absorption coefficient of 0.964 mM^{-1} upon hydrolysis of the ester bond (Hummel, 1959). The concentration of an enzyme stock was then calculated from the known specific activity of chymotrypsin for BTEE hydrolysis at pH 7.0 (1750 nmol hydrolyzed per minute per mole of chymotrypsin at pH 7.0). Previous work (Brady et al., 1990) has shown BTEE to be a classical substrate with k_{cat} = 32.2 s^{-1} and K_m = 11.5 μM under our assay conditions at pH 7.0.

Spectrophotometric Assay of Succinylalanylalanylprolylphenylalanine p-Nitroanilide. Succinylalanylalanylprolylphenylalanine *p*-nitroanilide (SAAPFpNA) was dissolved in 50% (v/v) H_2O/CH_3CN to 50 mM concentration. Aliquots were added to 1 mL of buffer A to achieve SAAPFpNA concentrations of 25–500 μM. Chymotrypsin was added to 30 nM, and the absorbance at 412 nm was observed until hydrolysis was complete. A molar extinction coefficient of 7958 M^{-1} was calculated from the net changes in absorbance at 412 nm. Michaelis–Menton kinetic constants of K_m = 30 μM and k_{cat} = 32 s^{-1} were obtained from the initial velocities.

pH-Stat Assays of Ester Substrates. Assays were conducted in 6.0-mL vials containing 2.0 mL of buffer B, with stirring provided by a magnetic flea. Substrate was added in acetonitrile such that all the assays contained less than 5% (v/v) organic solvent, and the starting pH was adjusted to 7.0 by addition of small aliquots of 100 mM NaOH or 100 mM HCl. Reactions were initiated by addition of enzyme, and the pH was maintained at 7.00 by the addition of NaOH titrant at a concentration of 1–20 mM as required for each particular substrate. Addition of titrant and recording of volume added vs time were performed automatically by a Radiometer titrator 11.

Plots of titrant added vs time were transformed to plots of velocity vs substrate concentration by the Basic program PHSTAT (available in the supplementary material) which calculates velocities by a numerical differentiation of the titrant added and calculates the substrate concentration by accounting for its conversion to product and dilution by titrant. Three to five such "progress curves" were obtained for each substrate, different starting substrate concentrations being used in order to confirm that product inhibition was not distorting the assumed Michaelis–Menton kinetics.

The kinetic constants k_{cat} and K_m were derived from these progress curves by directly fitting the Michaelis–Menton curve to the V vs S plot by nonlinear regression methods.

Ninhydrin Assay of Amide Substrates. Ammonia released upon hydrolysis of amide substrates was detected by a variation of the method of Stein and Moore (1948). One gram of ninhydrin was dissolved with stirring in 25 mL of 200 mM sodium citrate buffer (pH 5.0) containing 1.6 mg of $SnCl_2$/mL plus 25 mL of 2-ethoxyethanol. The solution was flushed with nitrogen for 10 min prior to use. This reagent was prepared fresh for each day of assays.

To measure ammonia content, a 50-μL aliquot of sample or standard solution was added to 0.5 mL of ninhydrin reagent. These mixtures were immersed in boiling water (with a loose cover to minimize evaporation) for 20 min, then 1 mL of water/2-propanol (1:1) was added, and absorbances at 570 nm were measured. Standard curves were linear between 0 and 250 nmol of NH_4^+/aliquot.

To measure amide hydrolysis, a concentrated chymotrypsin stock ([E] $\approx$ 1.5 mM) was prepared, and 10–50 μL of this was added to buffer A containing amide substrate (1–40 mM) to give a total volume of 500 μL. At intervals of 2–20 min (depending on the reaction rate), 50-μL aliquots were removed, and ammonia content was measured as described above. Plots of ammonia concentration vs time were linear, and rates of ammonia production were normalized by the amount of chymotrypsin in the reaction. All assays were conducted such that less than 20% of the total substrate was consumed during the reaction.

Inhibition Assays

Measurement of K_i. A chymotrypsin/BTEE assay was prepared as described above with an enzyme concentration of about 30 nM, with hydrolysis followed on a chart recorder at a speed of 5–10 cm/min. Shortly after initiation of the reaction, an aliquot (1–10 μL in acetonitrile) of inhibitor was

added, and the effect on the reaction rate was observed. Most of the inhibitors studied were "fast" in their action, and addition of inhibitor caused an immediate decrease in the reaction rate. A series of 6–10 such assays were done with varied inhibitor concentration. Data were expressed as the ratio of inhibited velocities to the control velocity in the absence of inhibitor, $f = V/V_0$. Plots of $1-f$ vs [I] were hyperbolic, and K_i was evaluated from a direct fit of an equilibrium binding hyperbola to a plot of $1 - f$ vs [I]:

$$1 - f = [I]/\{[I] + K_i(1 + [S]/K_m)\}$$

Progress Curves. Measurement of K_i of slow-binding inhibitors requires a reduction in enzyme concentration so as to prevent depletion of substrate prior to attainment of inhibitory equilibrium. Progress curves were conducted in 1.0 mL of buffer A containing 500 μM BTEE, 2.5% acetonitrile, and 1–5 nM chymotrypsin. The reaction was monitored spectrophotometrically at 256 nm, and after it was clear that the assay was proceeding normally, an aliquot of inhibitor was added. Hydrolysis of BTEE gradually slowed until enzyme, inhibitor, and substrate attained a steady-state equilibrium, with the reaction rate being linear but with reduced slope. Reaction conditions were adjusted so that total utilization of substrate was less than 30%.

Data from progress curves were fit to eq 1a (Cha, 1975) with a nonlinear least-squares regression algorithm (RS1, BBN Software Products Corp.). Values of k' from four to six progress curves were plotted vs inhibitor concentration [I]. k_{on} was evaluated from the slope (eq 1b), and k_{off} was evaluated from the intercept of this plot. K_i was calculated from each progress curve according to eq 1c. K_i is averaged for the four to six progress curves, and k_{off} is calculated as $K_i k_{on}$.

$$P(t) = V_{ss}t + (V_0 - V_{ss})[1 - \exp(-k't)]/k' \quad (1a)$$

$$k' = k_{off} + k_{on}[I]/(1 + [S]/K_m) \quad (1b)$$

$$K_i = [I]V_{ss}/(V_0 - V_{ss})(1 + [S]/K_m) \quad (1c)$$

Dissociation of E–I Complex. An independent measure of k_{off} was made by observing the dissociation of purified E–I complex. A miniature gel-filtration column was prepared (0.4 cm × 5 cm in a 1-mL disposable syringe) with G-15 Sephadex (Penefsky, 1979). The column was equilibrated with buffer A at 4 °C and then centrifuged in a table-top clinical centrifuge for 30 s to remove excess buffer. An enzyme stock of 1–5 μM concentration was treated with sufficient inhibitor to bind more than 95% of the enzyme. The enzyme/inhibitor mixture was allowed sufficient time (>20 min) to attain equilibrium and then was chilled to 4 °C. An aliquot of 100 μL of this mixture was added on top of the column, and the column was centrifuged in a table-top centrifuge for 90 s.

Free inhibitor (molecular weight 300–400) is retained in the gel matrix, while E–I complex (molecular weight 25 000) passes through. An aliquot of the eluant was added to a standard assay, and recovery of the enzyme activity was observed. A fit of the recovery curves to eq 2 yielded k_{off}.

$$P(t) = V_{ss}t + (V_0 - V_{ss})[1 - \exp(-k_{off}t)]/k_{off} \quad (2)$$

In some experiments, the E–I complex was diluted into buffer without substrate; then, aliquots of this diluted E–I complex were added to a standard assay at known time intervals. Plots of $\ln [(A_\infty - A)/(A_\infty - A_0)]$ vs time (A = activity; A_0 = activity at $t = 0$; A_∞ = activity after complete dissociation of E–I) were linear with slopes of $-k_{off}$.

Kinetics by Proflavin Displacement. The dye proflavin has found numerous applications in studies of chymotrypsin/ligand binding kinetics and equilibria on the basis of the shift in the absorption maximum of proflavin upon binding to chymotrypsin (Himoe et al., 1969; Fersht & Requena, 1971b; Faller & LaFond, 1971; Schultz et al., 1977; Kennedy & Schultz, 1979; Kuramochi & Nakata, 1979). Conditions were found for which displacement of proflavin from the active site of chymotrypsin by peptidyl trifluoromethyl ketones could be followed spectrophotometrically, and the technique was applicable both to slow-binding and rapidly equilibrating inhibitors.

To provide as much continuity in technique as possible, all inhibitors were tested on the same day with identically prepared stock solutions. Inhibitor solutions were prepared by diluting concentrated stock solutions (in acetonitrile) into water. All aqueous inhibitor solutions were prepared 12 h prior to use to assure that hydration/dehydration equilibrium had been attained.

Chymotrypsin (60 mg) was dissolved in 60 mL of 100 mM potassium phosphate (pH 7.0), and concentration was determined by BTEE assay as 38.4 μM. Proflavin was added (210 μL of a 20.1 mM aqueous stock) to a final concentration of 70.0 μM. The kinetic runs were started by addition of 5 μL of aqueous inhibitor to 500 μL of the chymotrypsin/proflavin mixture. Mixing times of less than 3 s were uniformly achieved. The absorbance at 465 nm was observed to decrease, and when it reached a stable minimum value, the kinetic run was terminated. Each inhibitor was examined at five to eight different concentrations ranging from 7 to 2000 μM, with higher inhibitor concentrations being required for weaker inhibitors. Acetonitrile originating from the inhibitor stocks was never present in the proflavin/enzyme mixture in excess of 1% v/v.

Calculation of the concentration of enzyme–inhibitor complex, [EI], from the absorbance at 465 nm was achieved with previously measured absorption coefficients of bound and unbound proflavin (Brady, 1989), the known dissociation constant of proflavin to chymotrypsin, and the mass balance of the total quantities of chymotrypsin, inhibitor, and proflavin, where A = absorbance at 465 nm, E_0 = total chymotrypsin present (38.4 μM), P_0 = total proflavin present (70 μM), I_0 = total inhibitor present, ϵ = absorption coefficient (465 nm) of proflavin[3] (15321 M^{-1}), ϵ' = absorption coefficient (465 nm) of chymotrypsin/proflavin complex (32449 M^{-1}), and K_p = chymotrypsin/proflavin dissociation constant (45.4 μM):

$$[E\cdot P] = (A - \epsilon P_0)/(\epsilon' - \epsilon) \quad (3a)$$

$$[P] = P_0 - [EP] = (P_0\epsilon' - A)/(\epsilon' - \epsilon) \quad (3b)$$

$$[E] = K_p[E\cdot P]/[P] = K_p(A - \epsilon P_0)/(P_0\epsilon' - A) \quad (3c)$$

$$\begin{aligned}[EI] &= E_0 - [E] - [E\cdot P] \\ &= [E_0(P_0\epsilon' - A)(\epsilon' - \epsilon) - K_p(A - \epsilon P_0)(\epsilon' - \epsilon) - \\ &\qquad (A - \epsilon P_0)(P_0\epsilon' - A)]/(P_0\epsilon' - A)(\epsilon' - \epsilon)\end{aligned} \quad (3d)$$

$$\begin{aligned}[I] &= I_0 - [EI] \\ &= [(I_0 - E_0)(P_0\epsilon' - A)(\epsilon' - \epsilon) + K_p(A - \epsilon P_0)(\epsilon' - \epsilon) + \\ &\qquad (A - \epsilon P_0)(P_0\epsilon' - A)]/(P_0\epsilon' - A)(\epsilon' - \epsilon)\end{aligned} \quad (3e)$$

$$\begin{aligned}K_i &= [E][I]/[EI] \\ &= \{K_p(A - \epsilon P_0)[(I_0 - E_0)(P_0\epsilon' - A)(\epsilon' - \epsilon) + \\ &\qquad K_p(A - \epsilon P_0)(\epsilon' - \epsilon) + (A - \epsilon P_0)(P_0\epsilon' - A)]\}/ \\ &\qquad (P_0\epsilon' - A)[E_0(P_0\epsilon' - A)(\epsilon' - \epsilon) - \\ &\qquad K_p(A - \epsilon P_0)(\epsilon' - \epsilon) - (A - \epsilon P_0)(P_0\epsilon' - A)]\end{aligned} \quad (3f)$$

K_i was found to be consistent for all inhibitor concentrations used, confirming that the small acetonitrile component of the

[3] Constants were evaluated at pH 7.0 as described in Brady (1989).

Table I: Summary of Kinetic and Equilibrium Constants for Peptidyl TFK Inhibitors

peptide	K_i (μM)	k_{on} (M^{-1} s^{-1})	k_{off} ($\times 10^3$ s^{-1})	method[a]
Ac-Leu-			0.330	eid
Phe	1.2	430	0.51	pc (BTEE)
	2.4 ± 1	720 ± 300	1.7 ± 0.6	pf
Ac-Val-	2.8			eq
Phe			8.0	eid
	4	1530	7.0	pc (BTEE)
	5 ± 1	1090 ± 120	5.7 ± 1.1	pf
Ac-Ala-	11			eq (BTEE)
Phe	14 ± 1	1230 ± 360	17 ± 3	pf
Ac-Gly-	18			eq (BTEE)
Phe	12 ± 2	2220 ± 300	34 ± 8	pf
Ac-Phe	17			eq (BTEE)
	13	>6900	>107	pc (BTEE)
	20 ±1	3010 ± 750	65 ● 20	pf
Ac-Leu-Np	0.87			eq
	0.63	810	0.5	pc (BTEE)
	1.1	1590	1.7	pc (SAAPFpNA)
	0.67 ± 0.4	1580 ± 300	1.0 ± 0.5	pf
Ac-Np	6.3			eq (SAAPFpNA)
		9800	62	pc (SAAPFpNA)
	12 ± 2	3840 ± 500	47 ± 7	pf

[a] Methods: eid, dissociation of E–I followed by recovery curves; eq, equilibrium K_i (substrate in parentheses); pc, progress curves; pf, proflavin displacement.

reactions was not interfering with the absorption characteristics of the proflavin dye.

Figure 1 shows a plot of [EI] vs time for Ac-Gly-Phe-CF_3. The initial rate of change of [EI] and the final value of [EI] are both seen to depend on inhibitor concentration. In most cases the inhibitor concentration was similar to the enzyme concentration, and a pseudo-first-order analysis could not be applied. The Fortran program SOKIN (see supplementary material) was used to simulate and fit a second-order reaction to the [EI] vs time data. The simulated curves, superimposed on the observed values in Figure 1, generally show excellent agreement with the observed data. k_{on} was evaluated both from the simulation and from the initial rate of formation of EI, and the values obtained were in good agreement. The average values and standard deviations of K_i, K_{on}, and K_{off} derived from these simulations are listed in Table I.

Effect of Enzyme Concentration on k_{on} of Ac-Phe-CF_3. Five enzyme stocks were prepared, and the concentrations, evaluated by BTEE assay, ranged from 6.5 to 118 μM. A 50-μL aliquot of a 19.9 mM aqueous proflavin stock was added to 10 mL of each enzyme stock. Kinetic runs were initiated by adding 5 μL of an Ac-Phe-CF3 solution to 500 μL of each of these mixtures while the change in absorbance at 465 nm was being monitored. Data were analyzed as described above. The observed association rates (Table II) are the average values obtained from three runs at 38 < [I] < 175 μM.

Results

Inhibition Kinetics and Equilibria. The constants K_i, k_{on}, and k_{off} for each peptidyl TFK inhibitor as measured by several techniques are summarized in Table I. K_i for this series of

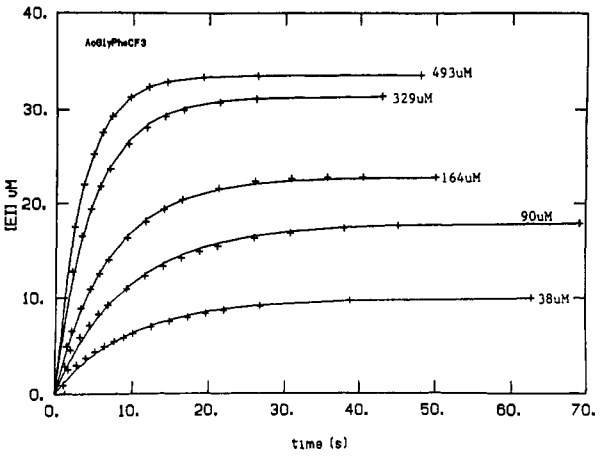

FIGURE 1: Kinetics of formation of chymotrypsin–Ac-Gly-Phe-CF_3 complex, by proflavin displacement. Formation of enzyme–inhibitor complex is calculated from the time-dependent change in absorbance at 465 nm by the methods described in the text. The solid curves represent simulated second-order reaction kinetics using association rate constants and dissociation rate constants optimized by the Fortran program SOKIN (see Materials and Methods).

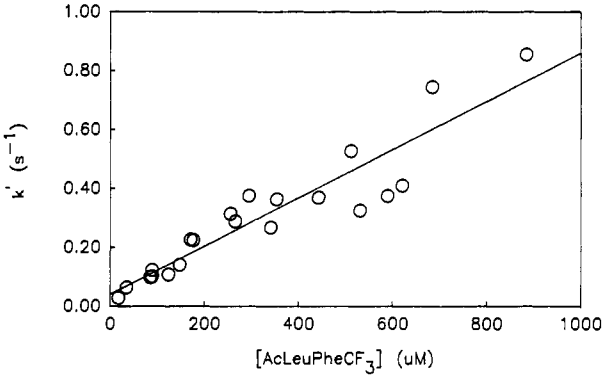

FIGURE 2: Evaluation of chymotrypsin–Ac-Leu-Phe-CF_3 association and dissociation kinetic constants from progress curves. k' is evaluated by fitting progress curves to eq 1a. Measurements were made in the presence of 350 μM BTEE so that $(1 + S/K_m) = 31.4$ μM.

inhibitors varies over a 30-fold range from 0.6 to 20 μM, k_{on} varies over a 20-fold range from 430 to 9800 M^{-1} s^{-1}, and k_{off} varies over a 300-fold range from 0.0003 to 0.1 s^{-1}. Results obtained by the different methods vary by 2–3-fold for K_i and k_{on} and up to 6-fold for k_{off}.

For the slow-binding inhibitor Ac-Leu-Phe-CF_3, k', as obtained by the method of Cha (1975), was in all cases first order with respect to inhibitor concentration. As shown in Figure 2, the plot of k' vs [I] (eq 1b) is linear at inhibitor concentrations as high as 885 μM. A limiting value of k' at high inhibitor concentrations was never observed with Ac-Leu-Phe-CF_3 or the other inhibitors of Table I to which the progress-curve technique was applicable (i.e., Ac-Val-Phe-CF_3, Ac-Leu-Np-CF_3, and Ac-Np-CF_3).

The rate of association of chymotrypsin with Ac-Phe-CF_3 is sufficiently fast that it cannot be measured with progress

Table II: Effect of Enzyme Concentration on the Apparent K_i, k_{on}, and k_{off} of Ac-Phe-CF_3 As Measured by Proflavin Displacement

[E] (μM)	av K_i (μM)[a]	av k_{on} (M^{-1} s^{-1})	av k_{off} (s^{-1})
0.008	13	>6900	>0.103 (Table III)
6.5	17.8 ± 6.1	4480 ± 1300	0.074 ± 0.02
13.8	32.9 ± 10.3	2720 ± 700	0.090 ± 0.03
35.3	34.2 ± 8.5	2580 ± 500	0.087 ± 0.03
59.9	35.4 ± 4.6	1960 ± 500	0.070 ± 0.03
117	39.6 ± 4.4	1180 ± 500	0.046 ± 0.03

[a] The listed values represent the average from three experiments at different inhibitor concentrations, with standard deviations.

Table III: Michaelis–Menten Kinetic Constants of Peptide Ester and Amide Substrates with Chymotrypsin

	methyl esters			amides		
peptide	k_{cat} (s^{-1})	k_m (μM)	k_{cat}/K_m (M^{-1} s^{-1})	k_{cat} (s^{-1})	K_m (mM)	k_{cat}/K_m (M^{-1} s^{-1})
Ac-Leu-Phe	22.8	16	1 430 000	0.572	31	18.2
Ac-Val-Phe	23.7	24.0	988 000	0.059	7.4	8.0
Ac-Ala-Phe	46.9	150	313 000	0.046	17.2	2.7
Ac-Gly-Phe	32.1	170	189 000	0.0048	9.0	0.53
Ac-Phe	59.7	329	181 000	0.033	45.1	0.73
Ac-Leu-Trp	3.3	2.6	1 269 000	0.482	17.7	27.2
Ac-Trp	44.8	31	1 445 000	0.0455	13.4	3.4

curves. In order to put a lower limit on k_{on} of Ac-Phe-CF_3 under progress-curve conditions, assays were conducted wherein hydrolysis of BTEE was initiated and then inhibitor was added with a mixing time of <6 s. Conditions for observing time-dependent inhibition were optimized by use of an expanded absorbance scale and fast chart speed. With inhibitor concentrations ranging from 81 to 810 μM, with inhibitor added from either aqueous or organic (CH_3CN) stock solutions, reproducible curvature in the postaddition trace was never observed.

Supposing that the progress-curve technique is not sufficiently sensitive to detect curvature when the inhibition reaction is 80% or more completed after mixing, then a limit for k_{on} can be calculated (Cha, 1975):

$$P(t) = V_{ss}t + (V_0 - V_{ss})[1 - \exp(-k't)]/k'$$

$$dP/dt = V_{ss} + (V_0 - V_{ss})\exp(-k't)$$

$$(dP/dt)_{t=0} = V_0 \qquad (dP/dt)_{t\to\infty} = V_{ss}$$

Immediately after mixing, time = t_m:

$$(dP/dt)_{t=t_m} = V_{t_m}$$

Since at $t = t_m$ the reaction is >80% complete, it follows that

$$V_{t_m} < V_0 - 0.8(V_0 - V_{ss})$$

$$\exp(-k't_m) < 0.2$$

so $k' > 0.27$ s^{-1}, where $t_m = 6$ s. If K_i ($=k_{off}/k_{on}$) is known, then a lower limit for k_{on} is

$$k_{on} > 0.27/\{K_i + [I]/(1 + [S]/K_m)\}$$

Using the observed values $K_i = 13$ μM, [I] = 810 μM, and $[S]/K_m = 31$, it follows that for Ac-Phe-CF_3 $k_{on} > 6900$ M^{-1} s^{-1}.

Effect of Enzyme Concentration on k_{on} of Ac-Phe-CF_3. With peptidyl aldehyde inhibitors of serine and thiol proteases, the free aldehyde, not the hydrate, is the reactive inhibitory species (Schultz et al., 1989). If the free trifluoromethyl ketone is the species which reacts with chymotrypsin, then the observed rate constant (k_{on}) might decrease at high enzyme concentration due to depletion of the ketone species. Therefore, the effect of enzyme concentration on k_{on} of Ac-Phe-CF_3 was studied as described under Materials and Methods and is summarized in Table II. These results show that the observed association rate decreases with increasing enzyme concentration.

Kinetics of Ester and Amide Substrates Corresponding to Inhibitors. It was of interest to compare the effect of P_2 substituents on inhibition kinetics to their effect on the catalytic reaction. Fourteen dipeptide methyl esters and amides were assayed by the techniques described above. Table III summarizes the Michaelis–Menton kinetic properties of these substrates.

The Michaelis–Menton kinetic constants of Ac-Phe, Ac-Ala-Phe, and Ac-Trp ester and amide substrates can be compared to measurements from past studies (Berezin et al., 1971; Foster & Niemann, 1955; Zerner et al., 1964; Bauer et al., 1976; Bender et al., 1964; Brouwer & Kirsch, 1982). Values from this study are generally consistent with past work, though there exists 6-fold variation in reported values for K_m of ester substrates.

Table IV: Differential Effect of Substituents on Catalysis: Hydrophobicity of the P_2 Subsite

substrate	P_2 side chain R	ΔG_R (kcal/mol)[a] ester	ΔG_R (kcal/mol)[a] amide	ΔG_{Roct} (kcal/mol)[b]
	Changes at P_2 in Ac-Xxx-Phe			
Ac-Gly-Phe	H	0	0	0
Ac-Ala-Phe	CH_3	−0.3	−1.0	−0.5
Ac-Val-Phe	$CH(CH_3)_2$	−1.0	−1.6	−1.3
Ac-Leu-Phe	$CH_2CH(CH_3)_2$	−1.2	−2.1	−1.8
	Changes at P_1 in Ac-Leu-Xxx			
Ac-Leu-Phe	phenyl	0	0	
Ac-Leu-Trp	indole	0.1	−0.2	
	Changes at P_1 in Ac-Xxx			
Ac-Phe	phenyl	0	0	
Ac-Trp	indole	−1.2	−0.9	

[a] $\Delta G_R = -RT \ln [(k_{cat}/K_m)_{PR}/(k_{cat}/K_m)_P]$, where P denotes the parent peptide (Ac-Gly-Phe) and R represents an added side chain. [b] From Hansch and Coates (1970). Gibbs free energy of transfer of group R from H_2O to octanol, equal to $-RT$ log (P_{OR}/P_O), where P_O and P_{OR} are the water/octanol partition coefficients of parent and R-substituted test compounds, respectively.

Hydrophobicity of P_2 Subsite. For a homologous series of compounds differing in some molecular portion R, the binding energy available for catalysis relative to a parent compound is

$$\Delta G_R = -RT \ln \{(k_{cat}/K_m)_{PR}/(k_{cat}/K_m)_P\}$$

where P denotes parent compound and PR denotes parent compound plus substituent R.

Table IV lists ΔG_R for the homologous series of substrates with varying P_2 side chains with Ac-Gly-Phe-OMe and Ac-Gly-Phe-NH_2 (R = H) as the parent compounds. The relative contributions of side chains R to catalysis, ΔG_R, are plotted with respect to the Gibbs free energy of transfer of R from water to octanol. ΔG_{Roct} (Figure 3). The slope of 0.75 indicates that the P_2 subsite provides a medium 75% as hydrophobic as octanol. A similar study of the P_1 subsite (Dorovskaya et al., 1972) demonstrated that the primary specificity pocket provides an environment 2.2 times more hydrophobic than octanol.

Changes due to substitutions at P_1 and P_2 are not always additive. In a comparison of Ac-Phe and Ac-Trp substrates, k_{cat}/K_m is enhanced by 1.0 kcal/mol due to the additional binding energy of the indole group relative to the phenyl group. However, in a comparison of Ac-Leu-Phe and Ac-Leu-Trp substrates, catalysis is enhanced by less than 0.2 kcal/mol by the same substitution. In this case, the enzyme appears unable to simultaneously utilize binding interactions at the P_1 and P_2 subsites.

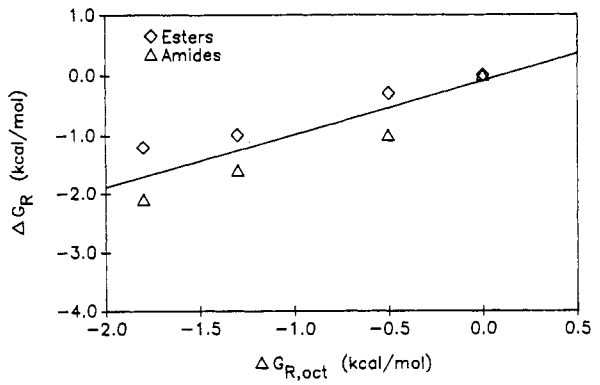

FIGURE 3: Hydrophobicity of the P_2 subsite. ΔG_{Roct} is the Gibb's free energy of transfer of a side-chain fragment from water to alcohol, and ΔG_R is the incremental change in $-RT \ln (k_{cat}/K_m)$ due to the same side-chain fragment.

Discussion

The studies described here were undertaken to determine the contribution of P_2 substituents of peptidyl TFK inhibitors to inhibition kinetics and equilibria and to gain a better understanding of the basis for the slow binding of some peptidyl TFK inhibitors to chymotrypsin. Before discussing the effect of P_2 substituents upon the kinetics of slow-binding inhibitors, it is necessary to define the reactive inhibitory species and the reaction sequence involved in inhibitor–chymotrypsin complex formation.

TFK Hydrate/Ketone Equilibrium. Since the slow association rate of Ac-Leu-Phe-CF_3 with chymotrypsin was first observed (Imperiali & Abeles, 1986), it has been considered that the very strong tendency for TFKs to form a ketone hydrate in aqueous solutions might be responsible for this kinetic behavior. An important assumption which is made in subsequent discussions is that the equilibria and kinetics of the trifluoromethyl ketone moiety will not be influenced by distant groups; i.e., the ketone functionality of Ac-Leu-Phe-CF_3 will behave in a manner identical with that of the ketone functionality of Ac-Phe-CF_3.

The inductive effect of the strongly electron-withdrawing trifluoromethyl group upon the adjacent ketone carbonyl causes the latter to become highly electrophilic. In aqueous solutions TFKs tend to be present almost entirely as the ketone hydrate, with a hydration constant defined as

$$K_h = [I_h]/[I_k][H_2O]$$

where $[I_h]$ = concentration of I present as hydrate and $[I_k]$ = concentration of I present as ketone. The ratio of ketone to hydrate in aqueous solution is 1/500 (K_h = 9.0 M^{-1}) for alkyl trifluoromethyl ketones (Allen & Abeles, 1989). The peptidyl TFKs possess an additional electron-withdrawing amido moiety on the α-carbon, and the ratio is expected to be smaller. Measurements of the ketone/hydrate ratio in *di*fluoromethyl ketones with and without the α-amido group (C. Govardhan, unpublished results) indicate that the α-amido group increases K_h by a factor of 9. Applying this same factor to TFKs gives K_h = 81 M^{-1}, I_h/I_k = 4500. This estimate of the hydrate/ketone ratio will be used in the following discussion.

It has been demonstrated for TFK inhibitors of cholinesterase (Allen & Abeles, 1989) that the inhibitor in its ketone form combines with the enzyme. Though we have not been able to apply the techniques used with cholinesterase to chymotrypsin, it is probable that chymotrypsin also reacts specifically with the ketone form. The data in Table II indicate that the observed association rate of Ac-Phe-CF_3 and chymotrypsin decreases with increasing enzyme concentration. This is consistent with reaction of the enzyme with the ketone form of the TFK, since at high enzyme concentrations the ketone form of the inhibitor may be consumed more rapidly than it is formed from the hydrate, with dehydration becoming rate limiting. This phenomenon will be discussed quantitatively after consideration of the reaction mechanism.

Proposed Mechanism of Inhibition. A two-step mechanism (Scheme I) is proposed which is analogous to the initial steps of the reaction of enzyme and substrate, and which has also been invoked to account for the reaction of serine proteases with aldehyde-based, TFK-based, and boronic acid based inhibitors (Stein et al., 1987; Kettner et al., 1988; Schultz et al., 1989). Evidence for the existence of the noncovalent intermediate (E·I) is seen in the decrease in k_{on} of Ac-Leu-Phe-CF_3 at high pH (Brady et al., 1989). With substrates the decrease of k_{cat}/K_m at high pH is due to decreasing stability of the E·S complex. By analogy, the decrease in k_{on} at high pH is most probably due to decreasing stability of E·I.

Scheme I

$$E + I \underset{k_{-1}}{\overset{k_1}{\rightleftharpoons}} E{\cdot}I \underset{k_{-2}}{\overset{k_2}{\rightleftharpoons}} E{-}I$$

$$K_{s,i} = [E][I]/[E{\cdot}I] \qquad K_i = [E][I]/[E{-}I]$$

It seems reasonable that $K_{s,i}$ should be similar to or larger in magnitude than K_s of an analogous amide substrate, which is in the range of 5–45 mM for the dipeptide substrates (see Table III, where for amide substrates $K_m = K_s$). Even if it is assumed that $K_{s,i}$ is as low as 1 mM, half-saturation of the enzyme by the *ketone form* of inhibitor would require inhibitor concentrations greater than 4 M. Since the maximum total inhibitor concentration used in any progress-curve experiment was 2.3 mM, linearity of the pseudo-first-order plots is entirely consistent with Scheme II.

Taking the hydration/dehydration equilibrium into account, the reaction of peptidyl TFKs with chymotrypsin is represented by Scheme II. In Scheme IIa, the formation of a Michaelis complex and the ensuing first-order covalent complex formation are combined into a single second-order reaction with a complex rate constant k_i. Scheme IIa therefore serves to describe the reaction kinetics under our experimental conditions, for which the inhibitor concentration is low and the reaction appears first-order in inhibitor concentration.

Scheme II

$$I_h \underset{k_h[H_2O]}{\overset{k_d}{\rightleftharpoons}} I_k + E \underset{k_{-1}}{\overset{k_1}{\rightleftharpoons}} E{\cdot}I \underset{k_{-2}}{\overset{k_2}{\rightleftharpoons}} E{-}I$$

Scheme IIa

$$I_h \underset{k_h[H_2O]}{\overset{k_d}{\rightleftharpoons}} I_k \underset{k_{-1}}{\overset{k_i[E]}{\rightleftharpoons}} E{-}I$$

$$k_i = k_1k_2/(k_{-1} + k_2)$$

If the formulation of the reaction of inhibitor with enzyme represented by Scheme II is accepted, then the observed association rates (k_{on}, Table I) need to be corrected to account for the concentration of the reactive ketone species. When $k_i[E] \ll k_h[H_2O]$, I_h and I_k are at equilibrium and the ratio of I_h/I_k = 4500, such that k_i = 4500 k_{on}. However, at a sufficiently large enzyme concentration, $k_i[E] \approx k_h[H_2O]$, the amount of ketone i_k decreases, and a larger correction factor is required:

$$k_i = 4500k_{on}k_d/(k_d - [E_0]k_{on}) \qquad (4)$$

Equation 4 (see Appendix for derivation of eq 4) states the

Table V: Kinetic and Equilibrium Constants of Peptidyl TFK Inhibitors Adjusted to TFK Ketone Concentration

peptide	k_{on} (M^{-1} s^{-1})[a]	k_i ($\times 10^{-6}$ M^{-1} s^{-1})[b]	K_i (nM)[c]
Ac-Leu-Phe	719	3.7	0.53
Ac-Val-Phe	1090	6.0	1.1
Ac-Ala-Phe	1230	7.0	3.2
Ac-Gly-Phe	2720	22	2.7
Ac-Phe	3010	27	4.5
Ac-Leu-Np	1580	9.6	0.15
Ac-Np	3840	47	2.7

[a] k_{on} obtained from kinetic measurements. [b] k_i as defined in Scheme IIa, eq 4. [c] K_i corrected to ketone concentration; i.e., $K_i = K_{i(obs)}/4500$.

relation between k_i and the observed k_{on} which holds at all enzyme concentrations. As an estimate of the dehydration rate, k_d, a value of 0.23 s^{-1} is used as the value which is most consistent with the k_{on} vs [E] data of Tables I and II. By use of this value of k_d and eq 4, k_i values can be calculated from k_{on}. The values for k_i and K_i, corrected for ketone concentration, are given in Table V.

In Figure 4, log k_i is plotted vs log (k_{cat}/K_m) for both esters and amides. A linear correlation with slope -0.69 ± 0.2 is observed. The negative slope occurs because those inhibitors which resemble the best substrates, and are tightest binding, also have the slowest association rates. Why do successively larger groups at the P_2 subsite decrease K_i, with k_i of Ac-Leu-Phe-CF_3 being 8-fold slower than k_i of Ac-Phe-CF_3? The larger leucine substituent at the P_2 subsite is known from crystallographic evidence (Brady et al., 1990) to form favorable hydrophobic contacts with His 57 and Ile 99 which stabilize the chymotrypsin–Ac-Leu-Phe-CF_3 complex. Similar interactions are assumed to account for the increase in k_{cat}/K_m of the dipeptide ester and amide substrates with larger side chains at the P_2 subsite. It therefore seems reasonable that the association rates of inhibitors with bulkier substituents at P_2 are slower due to the entropic requirement of simultaneously establishing these contacts at the P_2 subsite *and* attaining the necessary configuration of the reactive carbonyl and the catalytic residues of the enzyme. The relatively slow formation of proper contacts at the P_2 subsite contrasts with effects at the P_1 subsite, where substitution of the phenyl groups of Ac-Phe-CF_3 and Ac-Leu-Phe-CF_3 with the bulkier 2-naphthyl group of Ac-Np-CF_3 and Ac-Leu-Np-CF_3 *increases* k_i 2–3-fold. It is possible that the P_2 subsite is unique since substituents at P_2 directly affect the mobility of the catalytically essential His 57 imidazole.

It is useful to examine the nature of the complex rate constant, k_i. Under conditions for which $[I_k]$ is much smaller than $K_{s,i}$, the second-order rate constant for association, k_i is defined by eq 5.

$$k_i = k_1k_2/(k_{-1} + k_2) \quad (5)$$

Two limiting conditions can be considered: where $k_2 \gg k_{-1}$ so that $k_i \simeq k_1$: where $k_2 \ll k_{-1}$ such that $k_i = k_2/K_s$. What is a reasonable value for k_2? It is noted that the hydration rate of the peptidyl TFK in water at pH 7.0, as evaluated from the estimated dehydration rate (i.e., $k_h[H_2O] = K_hk_d[H_2O]$, where $K_h = 81$ M^{-1} and $k_d = 0.23$ s^{-1}), is approximately 1000 s^{-1}, while the rates of hydrolysis of the peptidyl esters and amides in water at pH 7.0 are approximately 10^{-8} and 10^{-12} s^{-1}, respectively (see Table VII). The rates of acylation of chymotrypsin in dipeptide ester and amide substrates are generally between 10^4 and 10^{-2} s^{-1} [Brady (1989) and references cited therein]. If the rate of nucleophilic addition of chymotrypsin to TFKs (k_2) relative to the rate of reaction with water is increased to the same extent as the rate of acylation by esters and amides, then k_2 can be as high as 10^{15} s^{-1}. Also,

Table VI: Association Rate Constants (k_1) for Chymotrypsin and Substrates

substrate	k_1 ($\times 10^{-6}$ M^{-1} s^{-1})	ref
N-(furylacryloyl)-L-tryptophanamide	6.2	Hess et al. (1970)
N-acetyl-L-phenylalaninamide	60	Hess (1971)
N-acetyl-L-tryptophan *p*-nitrophenyl ester	130	Hirohara et al. (1977)
N-acetyl-L-tryptophan *p*-nitrothiophenyl ester	240	Hirohara et al. (1977)
N-acetyl-L-tryptophan methyl ester	11	Brouwer and Kirsch (1982)
N-(methoxycarbonyl)-L-tryptophan *p*-nitrophenyl ester	89	Brouwer and Kirsch (1982)

Table VII: k_{noncat} and k_{cat}/K_m for Ac-Leu-Phe Ester and Amide Hydrolysis

reactant	k_{noncat} (s^{-1})[a]	k_{cat}/K_m (M^{-1} s^{-1})[b]	K_{tx} (M)[c]	$K_{i,k}$ (M)[d]	$\Delta G_i^\circ/\Delta G_{tx}^\circ$[e]
ester[f]	7.6×10^{-8}	1425000	5×10^{-14}	5×10^{-10}	0.70
ester[g]	9.5×10^{-9}	1425000	7×10^{-15}	5×10^{-10}	0.66
amide[h]	9.9×10^{-12}	18	5×10^{-13}	5×10^{-10}	0.76

[a] Rates are hydroxide-dependent rates, k_{OH^-}, applied at pH 7.0. [b] k_{cat}/K_m and $K_{i,k}$ apply to Ac-Leu-Phe-R, where R = methyl ester, amide, or TFK as appropriate. [c] $K_{tx} = k_{noncat}/(k_{cat}/K_m)$. [d] $K_i = [I_k]\cdot[E]/[E\text{-}I]$ from Table V. [e] $\Delta G_i^\circ = -RT \ln K_i$. $\Delta G_{tx}^\circ = -RT \ln K_{tx}$. [f] Hydroxide-dependent rate of hydrolysis of *N*-acetyl-L-phenylalanine methyl ester, from Bender et al. (1964). [g] Hydroxide-dependent rate of hydrolysis of methyl acetate at pH 7, from Bender et al. (1964). [h] Rate of hydrolysis of acetamide, from Yamana et al. (1972).

Hammet plots of log (k_{cat}/K_m) for each of the substrates vs σ of the group attached to the carbonyl (i.e., $-NH_2$, $-OMe$, and $-CF_3$, with Hammett coefficients σ_p of -0.57, -0.28, and 0.53, respectively; values are from tables in March 1985) predict rates of nucleophilic attack on the carbonyl of approximately 10^{15} s^{-1}.

These arguments suggest that the attack of the serine hydroxyl on the properly positioned TFK carbonyl is extremely facile. A similar conclusion was reached by Thompson (1973) regarding the rate of attack of the serine hydroxyl of elastase on the properly positioned aldehyde carbonyl of peptidyl aldehyde inhibitors. This suggests that the measured second-order rate constant for association of the peptidyl TFKs with chymotrypsin is k_1, the rate of formation of the E·I complex. The association rate constants (k_1) reported in Table V were measured at pH 7.0. At the pH optimum (pH 8.0), these rate constants will be approximately 2-fold larger, so that k_i ($=k_1$) ranges from 7×10^6 to 94×10^6 M^{-1} s^{-1} for the series. Table VI presents the association rate constants reported for chymotrypsin and various substrates. Comparisons are best limited to amide and simple ester substrates since Brouwer and Kirsch (1982) and Hirohara et al. (1977) observe that large hydrophobic groups at the P_1' subsite (e.g., *p*-nitrophenyl) induce significantly faster association rates. Chymotrypsin is seen to associate with the peptidyl TFK inhibitors at rates very similar to those observed with substrates.

We shall next compare the inhibition equilibrium constants, K_i (Table V), to k_{cat}/K_m of the corresponding substrates. For an ideal transition state analogue inhibitor, a plot of log K_i vs log (k_{cat}/K_m) should be linear (Wolfenden, 1976;; Thompson & Bauer, 1979; Bartlett & Marlowe, 1983). Plots of log K_i of the peptidyl TFK inhibitors vs log (k_{cat}/K_m) of esters and amides (Figure 5) are linear with slopes of 0.65 ± 0.2. These peptidyl TFK inhibitors are about 65% as effective as substrates in utilizing binding energy derived from increasing

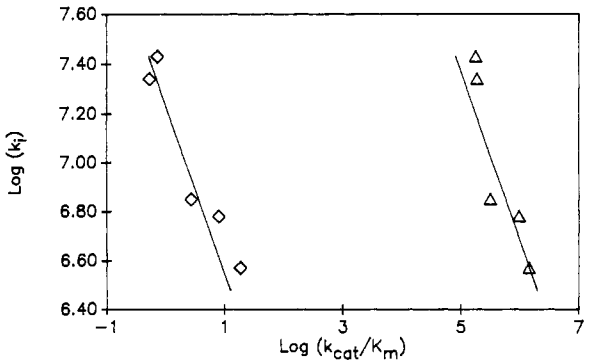

FIGURE 4: Comparison of rate constant for inhibition, log k_i, to log (k_{cat}/K_m) for homologous dipeptide methyl esters, amide, and trifluoromethyl ketones with aliphatic side chains at position P_2. (◇) Esters; (△) amides.

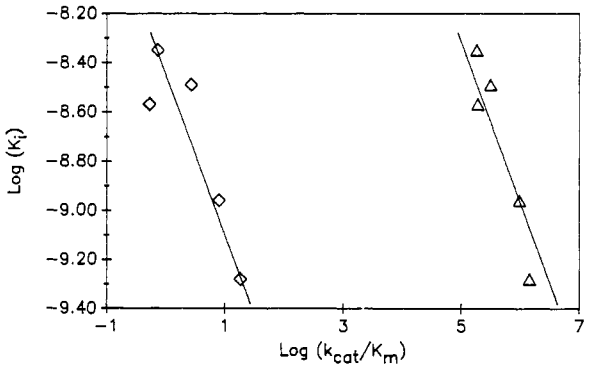

FIGURE 5: Comparison of equilibrium constant of inhibition, log K_i, to log (k_{cat}/K_m) for homologous dipeptide methyl esters, amide, and trifluoromethyl ketones with aliphatic side chains at position P_2. (◇) Esters; (△) amides.

hydrophobicity of the P_2 side chain.

The stability of an enzyme–transition state analogue inhibitor complex is related to the enzyme-catalyzed rate acceleration for an analogous substrate (Wolfenden, 1976):

$$K_{tx} = k_n/(k_{cat}/K_m)$$

where k_n = the noncatalytic reaction rate and $K_{tx} = K_i$ of an ideal transition-state analogue. The dissociation constant for an enzyme and an ideal transition state analogue inhibitor may therefore be expected to be equal to the rate acceleration provided by the enzyme relative to the noncatalyzed rate.

In Table VII, catalytic and noncatalytic rates of ester and amide hydrolysis are compared. Noncatalytic rates are for the hydroxide-dependent hydrolysis corrected to pH 7. K_{tx} is 4–5 orders of magnitude smaller than the observed K_i (i.e., K_i based on TFK ketone, $[I_k][E]/[E–I]$), corresponding to 5–8 kcal/mol of binding energy available for catalysis but not available for binding of the analogous TFK inhibitor. Only 65–75% of the theoretical binding energy between chymotrypsin and the transition state of the Ac-Leu-Phe substrates appears in binding to Ac-Leu-Phe-CF_3 (similar ratios are obtained for the other peptidyl TFK inhibitors of Table V), in agreement with conclusion reached from the plot of K_i vs k_{cat}/K_m. An ideal transition state analogue inhibitor based on the Ac-Leu-Phe structure should have a dissociation constant (K_{tx}) of less than 1 pM.

Given the general similarity of the chymotrypsin–Ac-Leu-Phe-CF_3 crystallographic model to other serine protease–transition state analogue models (α-lytic protease–tBocAla-Pro-boro-Val; Bone et al., 1987; SGPaseA–chymostatin, Delbaere & Brayer, 1985), it would be interesting to determine how closely other transition state analogue inhibitors approach the theoretical K_i. Partial answers to this question are available. Thompson (1973) observed that the inhibitory potency of two aldehyde-based inhibitors of elastase increased by 0.74 times the change in k_{cat}/K_m observed in analogous substrates. A slope of 1.3 was reported for a comparison of K_i of peptidyl TFKs and V/K for peptidyl p-nitroanilide substrates for elastase (Stein et al., 1987). Such studies are not yet reported for the peptidyl boronic acid inhibitors of serine proteases, though reported inhibition constants (Kettner & Shenvi, 1984) are similar to the inhibition constants of the peptidyl trifluoromethyl ketones (K_i based on free ketone, I_k). Correlations of log K_i vs log (k_{cat}/K_m) with slope greater than 1.0 (Bartlett & Marlowe, 1983; Stein et al., 1987) may indicate the presence of strong interactions between enzyme and inhibitor which are in addition to those interactions which characterize the enzyme's reaction transition state.

Conclusions

Scheme II incorporates the ketone/hydrate equilibrium of trifluoromethyl ketones, proposes transient formation of an enzyme–inhibitor Michaelis complex, and accounts for the kinetic observations. It is proposed that the conversion of Michaelis (E·I) complex to covalent (E–I) complex is extremely fast, such that the observed reaction rates reflect the second-order association rates, k_1, of enzyme and inhibitor. The second-order rate constants for association of chymotrypsin with the peptidyl TFK inhibitors, derived according to Scheme II (Table V), are similar to values observed with comparable substrates (Table VI).

In a homologous series of dipeptidyl TFK inhibitors, the rate constants for association with chymotrypsin decrease with increasing bulk of the P_2 side chain, indicating that formation of hydrophobic van der Waals interactions at the P_2 subsite, while favorable toward catalysis, is a relatively slow process. In the case of substrates, which are generally present at millimolar concentrations, the second-order association rates are easily sufficient to allow rapid attainment of steady state. In the case of the trifluoromethyl ketones, the concentration of the reactive species is typically in the nanomolar range. In this concentration range, slow binding is apparent only for those inhibitors which must form numerous van der Waals contacts at the P_2 subsite and which, therefore, have especially slow second-order association rate constants. Since these inhibitors bind more tightly than the faster associating inhibitors, they are generally present at lower concentrations, thereby magnifying the slow-binding effect.

A linear correlation is observed between the hydrophobicity of the P_2 substituent of dipeptide substrates and K_{cat}/K_m. This correlation suggests that the P_2 subsite environment is about 0.75 times as hydrophobic as octanol. Substituting leucine for glycine at the P_2 subsite of dipeptide substrates causes a 3-fold increase in K_m and an 8–30-fold increase in k_{cat}/K_m, illustrating how effectively chymotrypsin is able to direct the latent binding energy provided by additional hydrophobic substituents at P_2 toward enhanced catalysis. A linear relation with slope 0.65 was found between log K_i for dipeptidyl TFK inhibitors and log (k_{cat}/K_m) for the corresponding substrates. Thus, 65% of the binding energy available to stabilize the transition state of the catalytic process is available for binding of the TFK inhibitor.

Acknowledgments

We thank Nyla Spawn for assistance in preparation of the manuscript.

Appendix: Hydration/Dehydration Kinetics and a Derivation of Scheme II

This derivation uses the following symbols: I_k, I_h, and I_0, inhibitor as ketone or hydrate and total inhibitor, respectively; E_0, total enzyme; k_d, first-order rate constant for dehydration of I_h; k_h, second-order rate constant for hydration of I_k; k_{on}, apparent second-order rate constant for reaction between I_0 and enzyme; k_i, true second-order rate constant for reaction between I_k and enzyme; $[I_k]_t$, amount of I_k (or some other species) present at time = t. Typically, $t = 0$ or ss (steady-state interval).

Scheme IIa at Short Reaction Times. Consider the initial period of the reaction with enzyme when $[I_0] \approx [I_h]$, $[E{-}I] \approx 0$, and $[E] \approx [E_0]$:

$$d[I_k]/dt = [I_0]k_d - [I_k](k_h[H_2O] + k_i[E_0])$$

$$d[EI]/dt = k_i[I_k][E_0]$$

Rearranging, integrating, and solving for $[I_k]$

$$[I_k] = [I_k]_0\{1 - [E_0]k_i[1 - \exp(-k't)]/k'\} \quad (6)$$

where

$$k' = k_h[H_2O] + k_i[E_0] \quad (6a)$$

and

$$[I_k]_0 = [I_0]k_d/k_h[H_2O] \quad (6b)$$

Equation 6 indicates that $[I_k]$ is initially determined solely by its equilibrium with water, but upon addition of enzyme, $[I_k]$ falls with a time constant of k' to a steady-state value of

$$[I_k]_{ss} = [I]_0k_d/(k_h[H_2O] + [E_0]k_i) \quad (6c)$$

Since calculations of k_{on} from progress curves and proflavin displacement kinetics assume that $d[E{-}I]/dt = k_{on}[E][I]$, the observed k_{on} as defined for the initial moments of reaction is $(d[EI]/dt)/([E_0][I_0])$:

$$k_{on} = (k_ik_d/k_h[H_2O])\{1 - [E_0]k_i[1 - \exp(-k't)]/k'\} \quad (7)$$

Equation 7 implies that upon addition of enzyme there is a burst of E–I formation. The size of the burst is equal to the difference between the initial and steady-state inhibitor concentration:

$$\text{burst size} = [I_k]_0 - [I_k]_{ss} = [K_k]_0[E_0]k_i/(k_h[H_2O] + [E_0]k_i) \quad (8)$$

When $[E_0]k_i$ becomes large relative to $k_h[H_2O]$, the burst size approaches a maximum value of $[I_k]_0$ which, under conditions of the proflavin displacement experiments, is too small to be observed. Following the burst, formation of E–I continues at a steady-state rate which is the observed k_{on}:

$$k_{on} = k_ik_d/(k_h[H_2O] + [E_0]k_i)$$

Solving for k_i and substituting $k_h[H_2O]/k_d = 4500$ give

$$k_i = 4500k_{on}k_d/(k_d - [E_0]k_{on}) \quad (9)$$

Equation 9 allows the second-order rate constant, k_i, to be evaluated from the observed rate, k_{on}, independently of enzyme concentration. Equation 9 was derived by assuming short reaction times for which $[E{-}I] \approx 0$ and $[E] \approx [E_0]$. The observation that rate constants (k_{on}) calculated *both* from the initial rates of [E–I] formation *and* from the full-curve simulations of proflavin displacement reactions are in close agreement is believed to justify application of eq 9 to these measurements.

Supplementary Material Available

Synthetic methods and NMR spectral data for compounds in this paper and the Basic program PHSTAT and the Fortran program SOKIN (34 pages). Ordering information is given on any current masthead page.

References

Allen, K., & Abeles, R. H. (1989) *Biochemistry 28*, 8466.

Bartlett, P. A., & Marlowe, C. K. (1983) *Biochemistry 22*, 4618.

Bauer, C. A., Thompson, R. C., & Blout, E. R. (1976) *Biochemistry 15*, 1291.

Bender, M. L., Kezdy, F. J., & Gunter, C. R. (1964) *J. Am. Chem. Soc. 86*, 3714–3721.

Berzin, I. V., Kazanskaya, N. F., & Klyosov, A. A. (1971) *FEBS Lett. 15*, 121.

Bone, R., Shenvi, A. B., Kettner, C. A., & Agard, D. (1987) *Biochemistry 26*, 7609–7614.

Brady, K. (1989) Ph.D. Dissertation, Brandeis University.

Brady, K., Liang, T. C., & Abeles, R. H. (1989) *Biochemistry 28*, 9066–9070.

Brady, K., Wei, A., Ringe, D., & Abeles, R. H. (1990) *Biochemistry* (preceding paper in this issue).

Brouwer, A. C., & Kirsch, J. F. (1982) *Biochemistry 21*, 1302.

Cha, S. (1975) *Biochem. Pharmacol. 24*, 2177–2185.

Delbaere, L. T. J., & Brayer, G. D. (1985) *J. Mol. Biol. 183*, 89–103.

Dorovskaya, V. N., Varfolomeyev, S. D., Kazanskaya, N. F., Klyosov, A. A., & Martinek, K. (1972) *FEBS Lett. 23*, 122.

Faller, L. D., & LaFond, R. E. (1971) *Biochemistry 10*, 1033.

Fersht, A. R., & Requena, Y. (1971a) *J. Am. Chem. Soc. 93*, 7079.

Fersht, A. R., & Requena, Y. (1971b) *J. Mol. Biol. 60*, 279.

Foster, R. J., & Niemann, C. (1955) *J. Am. Chem. Soc. 77*, 1886.

Hansch, C., & Coats, E. (1970) *J. Pharm. Sci. 59*, 731.

Hess, G. P. (1971) *Enzymes (3rd Ed.) 3*, 228.

Hess, G. P., McConn, J., Ku, E., & McConkey, G. (1970) *Philos. Trans. R. Soc. London, Ser. B 257*, 89.

Himoe, A., Brandt, K. G., DeSa, R. J., & Hess, G. P. (1969) *J. Biol. Chem. 244*, 3483.

Hirohara, H., Phillipp, M., & Bender, M. L. (1977) *Biochemistry 16*, 1573.

Hummel, B. C. W. (1959) *Can. J. Biochem. Physiol. 37*, 1393.

Imperiali, B., & Abeles, R. H. (1986) *Biochemistry 25*, 3760.

Kennedy, W. P., & Schultz, R. M. (1979) *Biochemistry 18*, 349.

Kettner, C. A., & Shenvi, A. B. (1984) *J. Biol. Chem. 259*, 15106.

Kettner, C. A., Bond, R., Agard, D. A., & Bachovchin, W. W. (1988) *Biochemistry 27*, 7682.

Kuramochi, H., Nakata, H., & Ishii, S. (1979) *J. Biochem. 86*, 1403.

Liang, T. C., & Abeles, R. H. (1987) *Biochemistry 26*, 7603.

March, J. (1985) *Advanced Organic Chemistry*, 3rd ed., Wiley, New York.

Moore, S., & Stein, W. (1948) *J. Biol. Chem. 176*, 367.

Penefsky, H. S. (1979) *Methods Enzymol. 56*, 527.

Schecter, I., & Berger, A. (1967) *Biochem. Biophys. Res. Commun. 27*, 157.

Schultz, R. M., Konovessi-Panayotatos, A., & Peters, J. R. (1977) *Biochemistry 16*, 2194.

Schultz, R. M., Varma-Nelson, P., Ortiz, R., Kozlowski, K. A., Orawski, A. T., Pagast, P., & Frankfater, A. (1989) *J. Biol. Chem. 264*, 1497.
Stein, R. L., & Strimpler, A. M. (1987) *Biochemistry 26*, 2611.
Stein, R. L., Strimpler, A. M., Edwards, P. D., Lewis, J. J., Mauger, R. C., Schwartz, J. A., Stein, M. M., Trainor, D. A., Wildonger, R. A., & Zotolla, M. A. (1987) *Biochemistry 26*, 2682.
Thompson, R. C. (1973) *Biochemistry 12*, 47.
Thompson, R. C., & Bauer, C. A. (1979) *Biochemistry 18*, 1552.
Wolfenden, R. (1976) *Annu. Rev. Biophys. 5*, 271.
Yamana, T., et al. (1972) *Chem. Pharm. Bull. 20*, 881.
Zerner, B., & Bender, M. L. (1964) *J. Am. Chem. Soc. 86*, 3669.

Sequence of Sites on ATP-Citrate Lyase and Phosphatase Inhibitor 2 Phosphorylated by Multifunctional Protein Kinase (a Glycogen Synthase Kinase 3 Like Kinase)†

Seethala Ramakrishna, Guy D'Angelo, and William B. Benjamin*

Diabetes Research Laboratory, Department of Physiology and Biophysics, School of Medicine, Health Sciences Center, State University of New York, Stony Brook, New York 11794

Received March 19, 1990; Revised Manuscript Received May 15, 1990

ABSTRACT: Multifunctional protein kinase (MFPK) phosphorylates ATP-citrate lyase on peptide B on two sites, B_T and B_S, on threonine and serine, respectively, inhibitor 2 on a threonyl residue, and glycogen synthase at sites 2 and 3. The phosphorylation sites B_T and B_S of ATP-citrate lyase are dependent on prior phosphorylation at site A whereas site A phosphorylation is decreased by prior phosphorylation at sites B_T and B_S. To study the MFPK recognition sites and the site–site interactions, the amino acid sequences of ATP-citrate lyase peptide B and inhibitor 2 were determined and compared to each other and to glycogen synthase sites 3–5. The sequence of the tryptic peptide containing the two phosphorylation sites of peptide B is -Phe-Leu-Leu-Asn-Ala-Ser-Gly-Ser-Thr-Ser-Thr(P)-Pro-Ala-Pro-Ser(P)-Arg-, and the sequence of the MFPK phosphorylation site of inhibitor 2 is -Ile-Asp-Glu-Pro-Ser-Thr(P)-Pro-Tyr-. This inhibitor 2 site is identical with the site phosphorylated by glycogen synthase kinase $3/F_A$. These results suggest that at least some of the sites phosphorylated by MFPK (B_T of ATP-citrate lyase, Thr 72 of inhibitor 2, and sites 3b and 4 of glycogen synthase) contain a Ser/Thr flanked by a carboxyl-terminal proline. However, as MFPK did not phosphorylate a series of peptides containing the -X-Thr/Ser-Pro-X- sequence, this minimum consensus sequence is not sufficient for phosphorylation by MFPK. MFPK was able to phosphorylate glycogen synthase synthetic peptide only after it had first been phosphorylated by casein kinase II at site 5, supporting the hypothesis that the phosphorylation of natural substrates by MFPK depends on prior phosphorylation at other sites. ATP-citrate lyase sites B_T and B_S resemble glycogen synthase sites 3b and 3c, suggesting that MFPK recognizes a Ser/Thr in the following pattern: -Ser/Thr()-X-X-X-Ser/Thr(P)-. Additional evidence for this four amino acid spacing was obtained when the sequence about all three phosphorylation sites of ATP-citrate lyase was found to be -Thr(P)-Pro-Ala-Pro-Ser(P)-Arg-Thr-Ala-Ser(P)-, a configuration that resembles glycogen synthase sites 3b, 3c, and 4.

How insulin produces an increase in the phosphorylation of some proteins (Benjamin & Singer, 1974, 1975; Alexander et al., 1979; Ramakrishna & Benjamin, 1979, 1983a; Smith et al., 1980; Belsham et al., 1982; Petruzelli et al., 1984; Kahn et al., 1985; Denton, 1986) and a decrease in others (Engstrom, 1980; Huges et al., 1980; Lawrence et al., 1983, 1986; Denton, 1986) is not understood. Recent studies on ATP-citrate lyase phosphorylations have shed considerable knowledge on this problem. Insulin and isoproterenol both increase the phosphorylation of ATP-citrate lyase on peptide A whereas insulin decreases the phosphorylation of peptide B of ATP-citrate lyase, but isoproterenol increases its phosphorylation (Pucci et al., 1983; Ramakrishna et al., 1984). While looking for a protein kinase that phosphorylates peptide B of ATP-citrate lyase, a multifunctional protein kinase (MFPK)[1] that is similar to rabbit muscle glycogen synthase kinase/F_A was isolated from rat liver (Ramakrishna & Benjamin, 1981, 1985; Sheorain et al., 1985b). MFPK phosphorylates peptide B of ATP-citrate lyase and sites 2 and 3 of glycogen synthase (Ramakrishna & Benjamin, 1985; Sheorain et al., 1985b). MFPK was found to be an insulin-regulated kinase as insulin at physiological concentrations rapidly decreased its activity

† This work was supported by a grant from the American Heart Association, Suffolk Chapter, and Grant AM 18905 from National Institutes of Health. Preliminary reports of portions of these findings were presented at the 29th Annual Meeting of American Society for Cell Biology and 74th Annual Meeting of Federation of American Societies for Experimental Biology.

[1] Abbreviations: TPCK, L-1-(tosylamino)-2-phenylethyl chloromethyl ketone; MFPK, multifunctional protein kinase; TFA, trifluoroacetic acid; PKI, cAMP-dependent protein kinase inhibitor.

0006-2960/90/0429-7617$02.50/0